Heat and Mass Transfer in an Annular Vertical Porous Cylinder Considering Thermal Equilibrium with Internal Heat Generation

Suhrid Dev, Vivek Shrivastava, Pavan Badami, Mukesh Patil*

Abstract –The present study is an attempt towards understanding heat and mass transfer as well as fluid flow behavior inside an annular vertical cylinder with saturated porous media subjected to the case of natural convection. A study was carried out for constant heat generation within the medium with constant temperature boundary conditions. Variation of Nusselt Number and Sherwood number was studied with respect to Rayleigh-Darcy number, radius ratio and aspect ratio. This work was carried out using the Finite element method.

Keywords–finite element analysis, porous media, MATLAB, heat generation, porous annulus, heat and mass transfer.

1. INTRODUCTION

The porous medium is involved in numerous applications covering a large number of engineering disciplines. Study and research on natural convection in porous media enclosures have bloomed in the recent past due to their practical importance. Understanding of heat and fluid flow behavior in porous media will help to design systems in a better way so as to increase the efficiency of systems involving these media.

SUHRID DEV, Department of Mechanical Engineering, P. E. S. Institute of Technology, Bangalore, INDIA (email: suhridev@gmail.com).

VIVEK SHRIVASTAVA, Department of Mechanical Engineering, P. E. S. Institute of Technology, Bangalore, INDIA (email: vivekshrivastava2392@gmail.com).

PAVAN BADAMI, Department of Mechanical Engineering, P. E. S. Institute of Technology, Bangalore, INDIA (email: pavanbadami@gmail.com).

*MUKESH PATIL, Professor, Department of Mechanical Engineering, B.N.M. Institute of Technology, Bangalore, INDIA (email: patilmukesh@yahoo.com).

For instance, the study can help to find out the occurrence of maximum and minimum heat transfer rate with respect to geometrical parameters of cylindrical porous media, using which, the system can be designed so as to have maximum or minimum heat transfer rate. Nuclear reactor cooling is one application of convection in porous media with internal heat generation. The reactor bed can be modeled as a heat generating porous medium of cylindrical cross- section, quenched by a convection flow. An annular region is the most basic configuration that can be used to investigate a wide range of geometrical effects and boundary conditions. It can also be used to understand and implement results on complex configurations. There is abundant literature available for convection in porous saturated annular cylinder. Ahmed, Badruddin, Kanesan, Zainal, Ahamed [21] have worked on mixed convection in a porous annular cylinder with isothermal conditions on inner and outer wall, considering thermal non-equilibrium modeling. Havstad and Burns [17] used a perturbation method and a finite difference technique to analyze the heat transfer characteristics in a vertical annulus filled with a porous medium and presented correlations for the heat transfer in the annulus. Hickox and Gartling [18] studied natural convection flow in a vertical annular enclosure for a wide range of radius and aspect ratios, and also used an approximate analysis to obtain a closed form solution for the Nusselt number when the aspect ratio of the annulus is high. Work carried out by authors Reddy, Narasimhan [13] involves a study of the interplay between internal heat generation and externally driven natural convection inside a porous medium annulus using numerical methods. The axisymmetric domain is bounded with adiabatic top and bottom walls and differentially heated sidewalls. The generalized momentum equation with Brinkman–Darcy–Forchheimer terms and the local thermal non-equilibrium based two-energy equation model were solved to determine the flow and the temperature

distribution using the Finite Volume Method. Irfan [11] has studied free convection in an annular cylinder saturated with porous media having combined effect of natural convection and thermal radiation. His investigation included heat and mass transfer with respect to a plate and an annular cylinder subjected to variable temperature and isothermal temperature conditions, effect of viscous dissipation, heat transfer investigation including variable wall temperature for both equilibrium and non-equilibrium model. Natural convection by internal heat generation was studied in [16]. This study assumes local thermal equilibrium (LTE) to exist between the solid and fluid phases of the porous medium. 'Convection in porous media' by Bejan and Nield [4] was used to understand the basic concepts of heat transfer in porous media. 'Fundamentals of Finite Element Method for Heat and Fluid Flow' by Lewis, Nithiarasu and Seetharamu [3] was used to understand concepts in FEM and for formulation.

In our present study we have incorporated heat generation conditions for the thermal equilibrium model. Three cases were studied in our analysis. These have been depicted in fig. 2. The 3 cases that were examined as shown in fig. 2 are:

-Heat Generation on the top of the porous annulus.

-Heat Generation at the centre of the porous annulus.

-Heat Generation at the bottom of the porous annulus.

In each of these cases, the variation of the Nusselt number and the Sherwood number was studied with respect to Rayleigh-Darcy number, radius ratio and aspect ratio.

Nomenclature:

T; $\overline{T}$: Dimensional (°C) and non-dimensional temperatures respectively

C; $\overline{C}$: Dimensional and non-dimensional species concentration respectively

u, w = Velocity in r and z directions, respectively (m/s)

r, z= Cylindrical coordinates

R,Z=Non-dimensional cylindrical coordinates

H=Height of the cylinder

$L_{ref} = r_o - r_i$ =Reference/characteristic length

AR= aspect ratio= H/L_{ref}

Radr= radius ratio= $r_o - r_i/r_i$

Nu, Sh= average Nusselt and Sherwood numbers respectively

2. MATHEMATICAL MODELING AND FORMULATION

A two dimensional, axisymmetric model of a fluid-saturated vertical porous annular cylinder with an internal heat generating porous matrix was considered as the computational domain. Constant temperature boundary conditions were imposed. The vertical walls were differentially heated and maintained as hot left wall (T_h) and cold right wall (T_c). The horizontal walls were kept adiabatic. The analysis performed was for a steady, laminar, incompressible natural convection fluid saturating an annulus filled with a uniformly heat generating homogeneous isotropic porous solid matrix with uniform volumetric porosity. The convecting fluid and the heat generating solid matrix were considered to be in local thermal equilibrium. The Boussinesq approximation for linear density variation with local fluid temperature was assumed to be the cause of the buoyancy force in the convecting fluid.

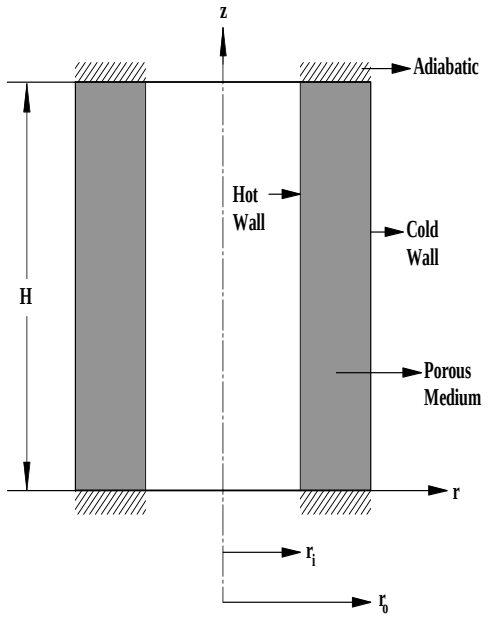

Fig 1. Porous Medium Embedded with Cylindrical Geometry.

VALIDATION:

Table 1

Ra*	Z-G. Du and E. Bilgen [16]	Walker et al.	Beckermann et al.	Shiralkar et al.	Present Study
50	1.978	1.98	1.981	no result	1.9632
100	3.091	3.097	3.113	3.115	3.0613
200	4.931	4.89	5.038	4.976	5.216

The results were cross-checked with previously published data for the case of natural convection inside the porous medium with heat generation. Further progress was made to predict the heat and fluid flow characteristics. The comparison of the Nusselt number values is shown in table 1, which establishes the accuracy of present method.

GOVERNING EQUATIONS:

The Continuity equation can be written as:

$$\frac{\partial(ru)}{\partial r} + \frac{\partial(rw)}{\partial z} = 0 \quad (1)$$

Where, u and w are the velocities in 'r' and 'z' directions respectively and defined as follows:

$$u = -\frac{K}{\mu}\frac{\partial p}{\partial r} \quad (2)$$

$$w = -\frac{K}{\mu}\left(\frac{\partial p}{\partial z} + \rho g\right) \quad (3)$$

The Momentum equation is as shown below:

$$\frac{\partial w}{\partial r} - \frac{\partial u}{\partial z} = r\frac{gK}{\nu}\left(\beta_T\frac{\partial T}{\partial r} + \beta_C\frac{\partial C}{\partial r}\right) \quad (4)$$

After substituting the non-dimensional parameters (as shown in table 1) in the momentum equation, we get:

$$\frac{\partial^2 \bar{\Psi}}{\partial Z^2} + R\frac{\partial}{\partial R}\left(\frac{1}{R}\frac{\partial \bar{\Psi}}{\partial R}\right) = RRa^*\left[\frac{\partial \bar{T}}{\partial R} + N\frac{\partial \bar{C}}{\partial R}\right] \quad (5)$$

The energy equation with heat generation is as shown below: $u\frac{\partial T}{\partial r} + w\frac{\partial T}{\partial z} = \alpha\left[\frac{1}{r}\frac{\partial \Psi}{\partial r}\left(r\frac{\partial T}{\partial r}\right) + \frac{\partial^2 \bar{T}}{\partial Z^2}\right] + \frac{q'''L_{ref}}{\rho C_p}$

(6)

The following non-dimensional parameters were defined and used:

Non dimensional radius $\bar{r} = \frac{r}{L_{ref}}$

Non dimensional height $\bar{z} = \frac{z}{L_{ref}}$

Non dimensional stream function $\bar{\Psi} = \frac{\Psi}{\alpha L_{ref}}$

Non dimensional temperature $\bar{T} = \frac{(T-T_\infty)}{(T_w-T_\infty)}$

Non dimensional concentration $\bar{C} = \frac{(C-C_\infty)}{(C_w-C_\infty)}$

Rayleigh-Darcy number $Ra^* = RaDa = \frac{(g\beta_T \Delta T K L_{ref})}{\nu\alpha}$

Where $Da = \frac{K}{L_{ref}^2}$ is the Darcy Number and $K = \frac{D_p^2 \Phi^3}{180(1-\Phi^2)}$ is the permeability of the medium

Thermal diffusivity for the medium can

be defined as: $\alpha = \frac{k}{\rho C_p}$

Lewis number $Le = \frac{\alpha}{D}$ where D is the diffusion coefficient

After substituting the non-dimensional parameters (as shown in table 1) in the energy equation with heat generation, we get:

$$\frac{1}{R}\left[\frac{\partial \bar{\Psi}}{\partial R}\frac{\partial \bar{T}}{\partial Z} - \frac{\partial \bar{\Psi}}{\partial Z}\frac{\partial \bar{T}}{\partial R}\right] = \left(\frac{1}{R}\frac{\partial}{\partial R}\left(R\frac{\partial \bar{T}}{\partial R}\right) + \frac{\partial^2 \bar{T}}{\partial Z^2}\right) + G \quad (7)$$

Where $G = \frac{q'''L_{ref}^2}{k(T_w - T_\infty)}$ is the non-dimensional heat generation.

L_{ref} =r_o-r_i=the thickness of the porous zone.

k =thermal conductivity of the medium.

q''' Is the volumetric heat generation within the medium.

The Concentration Equation can be shown as:

$$u\frac{\partial C}{\partial r} + w\frac{\partial C}{\partial z} = D\left\{\frac{1}{r}\frac{\partial}{\partial r}\left(r\frac{\partial C}{\partial r}\right) + \frac{\partial^2 C}{\partial z^2}\right\} \quad (8)$$

After substituting the non-dimensional parameters (as shown in table 1) in the concentration equation, we get:

$$\frac{1}{R}\left[\frac{\partial \bar{\Psi}}{\partial R}\frac{\partial \bar{C}}{\partial Z} - \frac{\partial \bar{\Psi}}{\partial Z}\frac{\partial \bar{C}}{\partial R}\right] = \frac{1}{Le}\left(\frac{1}{R}\frac{\partial}{\partial R}\left(R\frac{\partial \bar{C}}{\partial R}\right) + \frac{\partial^2 \bar{C}}{\partial Z^2}\right) \quad (9)$$

BOUNDARY CONDITIONS:

Constant temperature and species concentration values were specified on the hot and cold walls. The boundary conditions used for this case, taking into account heat generation within the medium, are as shown below:

At the inner wall of the annulus:

At r = r_i ; T = T_i ; C = C_i ; Ψ = 0

At the outer wall of the annulus:

At r = r_o ; T = T_∞ ;C = C_o ; Ψ = 0

The value of non-dimensional generation was specified as 0.1, to minimise time for execution of our program.

Applying the non-dimensional parameters (as shown in table 1) in the above equations results in the following non dimensional boundary conditions:

a) At the inner wall of the annulus:

At r = r_i; $\bar{T}=\bar{T}_i=1$; $\bar{C}=\bar{C}_i= 1$; $\bar{\psi} = 0$

b) At the outer wall of the annulus:

At r = r_o; $\bar{T}=\bar{T}_\infty=0$;$\bar{C}=\bar{C}_i= 0$; $\bar{\psi}= 0$

The average Nusselt number ($\overline{Nu}$) is calculated by using the relation as shown. The temperature gradient $\left(\frac{\partial \bar{T}}{\partial \bar{r}}\right)$ is evaluated using a 4-point polynomial fitting function along the nodes near the inner wall of the vertical porous annular cylinder.

$$\overline{Nu} = -\int_0^{\bar{z}} \frac{\partial \bar{T}}{\partial \bar{r}} \overline{\partial z} \quad (10)$$

3. SOLUTION METHODOLOGY

The solution of these governing equations gives the effect of several parameters on fluid flow and heat in porous media. In the present study, Finite Element Method (FEM) was used for all the case studies. The Galerkin's method was employed to convert the partial differential equations into matrix form of equations for an element.

Three cases were studied in our analysis. These have been depicted in fig. 2. The 3 cases that were examined as shown in fig. 2 are:

-Heat Generation on the top of the porous annulus.

-Heat Generation at the centre of the porous annulus.

-Heat Generation at the bottom of the porous annulus.

The computational domain bounded by the region of the porous wall was meshed as shown in each of the three cases shown fig. 2. The x coordinate values 0.2 to 1.2 represent the extreme values of non-dimensional radius. The y coordinate values 0 to 5 represent the extreme values of the non-dimensional height. The region consists of 1800 elements and 961 nodes.

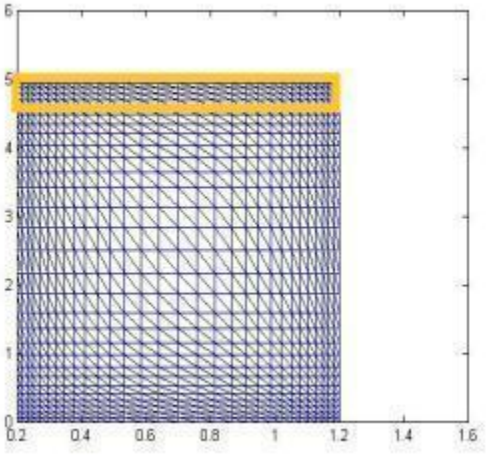

1. Heat generation zone defined on the top of the porous wall.

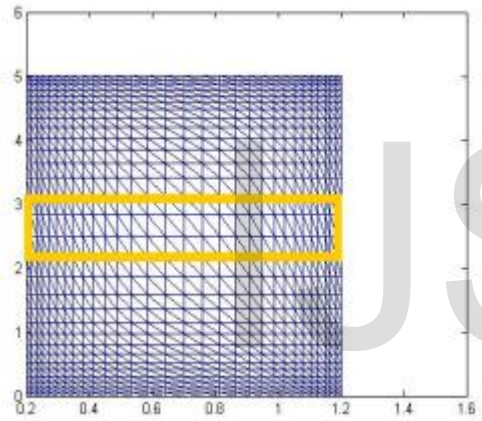

2. Heat generation zone defined at the centre of the porous wall.

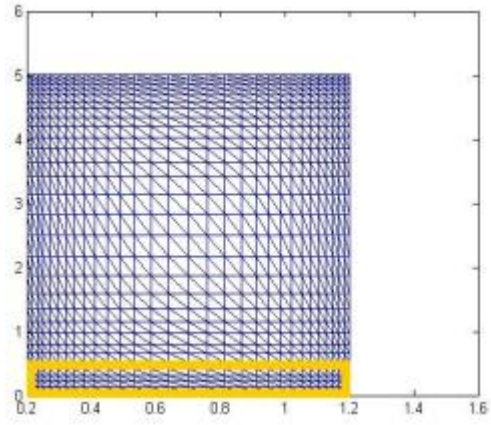

3. Heat generation zone defined at the bottom of the porous wall.

Fig. 2 Above is a schematic representation of the section of the porous wall after it has been meshed in each of the three cases that were examined.

4. RESULTS AND DISCUSSIONS:

ISOTHERMAL PLOTS OBTAINED FOR GG=0.1, Radr=Asp=1 at various Rayleigh-Darcy numbers:

TOP:

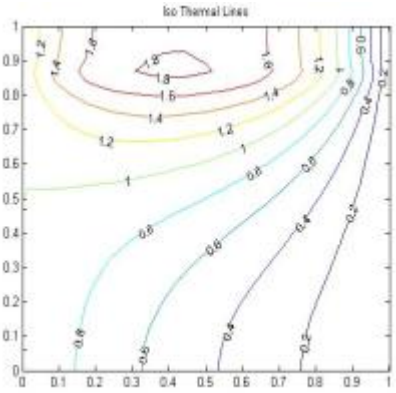

For Ra*=10

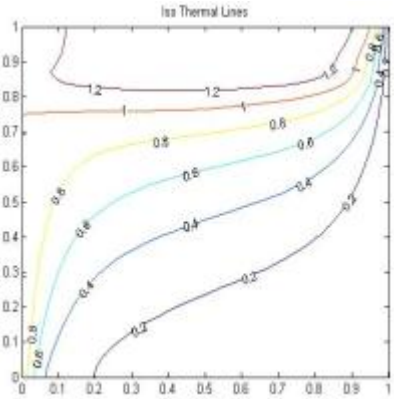

For Ra*=100

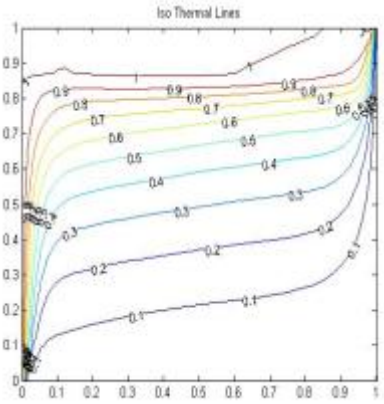

For Ra*=1000

CENTRE:

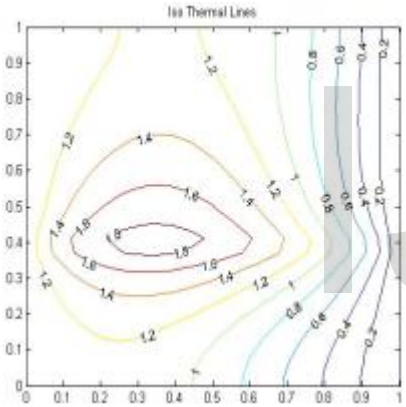

For Ra*=10

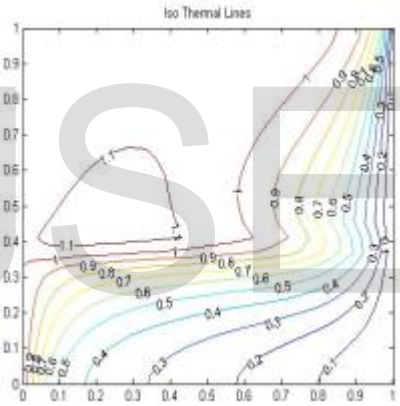

For Ra*=100

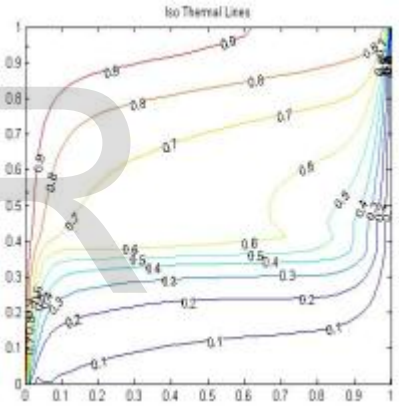

For Ra*=1000

BOTTOM:

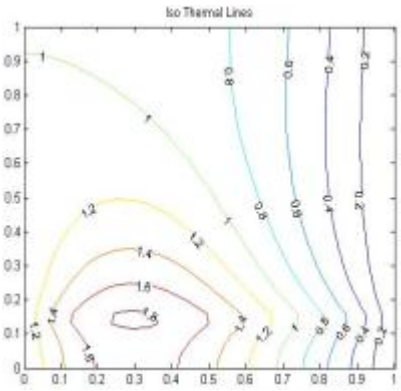

For Ra*=10

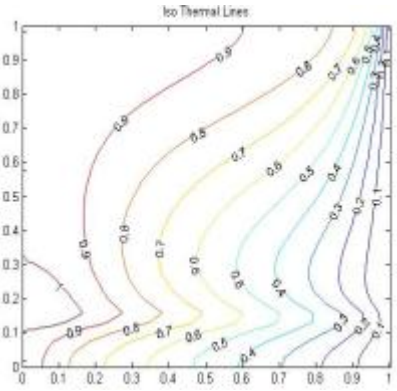

For Ra*=100

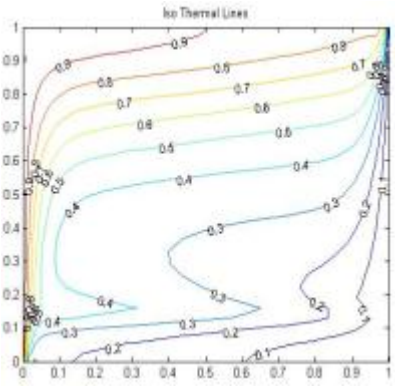

For Ra*=1000

Fig 3 Isotherms for various Rayleigh number considering generation on top, centre and bottom.

The variation in the isothermal lines can be seen in fig. 3 for various Rayleigh-Darcy numbers. One can clearly see how the isothermal profile from Ra*=10 (pure conduction) to Ra*=1000(pure convection) varies (in each of the cases) and how the profile changes as flow develops-from nearly vertical lines, parallel to the walls to nearly horizontal lines perpendicular to the walls. At low values of Ra*, it can also be seen that the isotherms localize and confine themselves to a region near the heat source. A region of the isothermal plot, located near the heat source remains parallel with the top wall, near the source, indicating that the flux associated with the heat generating source is in a direction perpendicular to the top walls and parallel to the hot and cold walls. As the value of Ra* was increased, it was observed that the isotherms began to accumulate and crowd near the hot wall. This indicated the development of stronger and higher thermal gradients near the hot wall due to a decrease in the thickness of the thermal boundary layer.

Fig. 4a shows the Nusselt number variation with respect to the Rayleigh-Darcy number for a value of Non-dimensional heat generation =0.1(Aspect Ratio=1, Radius Ratio=1). In this case, the Nusselt number variation with respect to the Rayleigh-Darcy number was found to be nearly constant in the range of Ra*=1 to Ra*=75, indicating that the heat transfer rate wasn't affected much in the pure conduction case (i.e at low values of Ra*). As the Rayleigh-Darcy was increased beyond Ra*=75, the Nusselt number started increasing exponentially. This indicated that better fluid circulation and higher buoyancy effects in the flow improved the rate of heat transfer drastically. Fig. 4b shows the effect of a positive buoyancy ratio on the plot obtained in 4a. The Nusselt number was found to increase. The thermally induced buoyancy forces were being assisted by the mass induced buoyancy forces for the case of N=1. In both 4a and 4b, the Nusselt number was found to be highest for the case of heat generation at the bottom. This is due to the fact that the fluid circulation is enhanced as the heat source moves down, allowing circulation of the entire fluid present within the cavity. As the heat source is shifted upwards, there is a tendency for the fluid to become stagnant near the bottom. As a result of which, convection induced fluid circulation is not at its full potential, and consequently, the heat transfer rate diminishes.

In fig. 5, for a constant value of non-dimensional heat generation=0.1, a constant value of aspect ratio=5 and a constant Rayleigh-Darcy number of 600, the average Nusselt number was found to increase with an increase in radius ratio. This result follows from the fact that with increasing radius ratio, the annulus width increases, and the fluid volume associated with the strong temperature and velocity gradients near the inner boundary increases. Again, the Nusselt number was found to be at its highest when the heat generating zone was located at the bottom of the porous wall and decreased as the source shifted upwards.

In fig. 6, it is observed, that, for a constant value of radius ratio and Rayleigh-Darcy number, the average Nusselt number was found to decrease with an increase in aspect ratio. As aspect ratio increases, the thermal boundary layer increases in thickness due to reduced fluid density. Increase in the thermal boundary layer thickness and reduced fluid density cause a reduction in the heat transfer by convection, thereby, leading to a reduced Nusselt number. Again, the Nusselt number was found to be maximum for the case of heat generation on the bottom of the porous wall, and gradually decreased as the source shifted upwards.

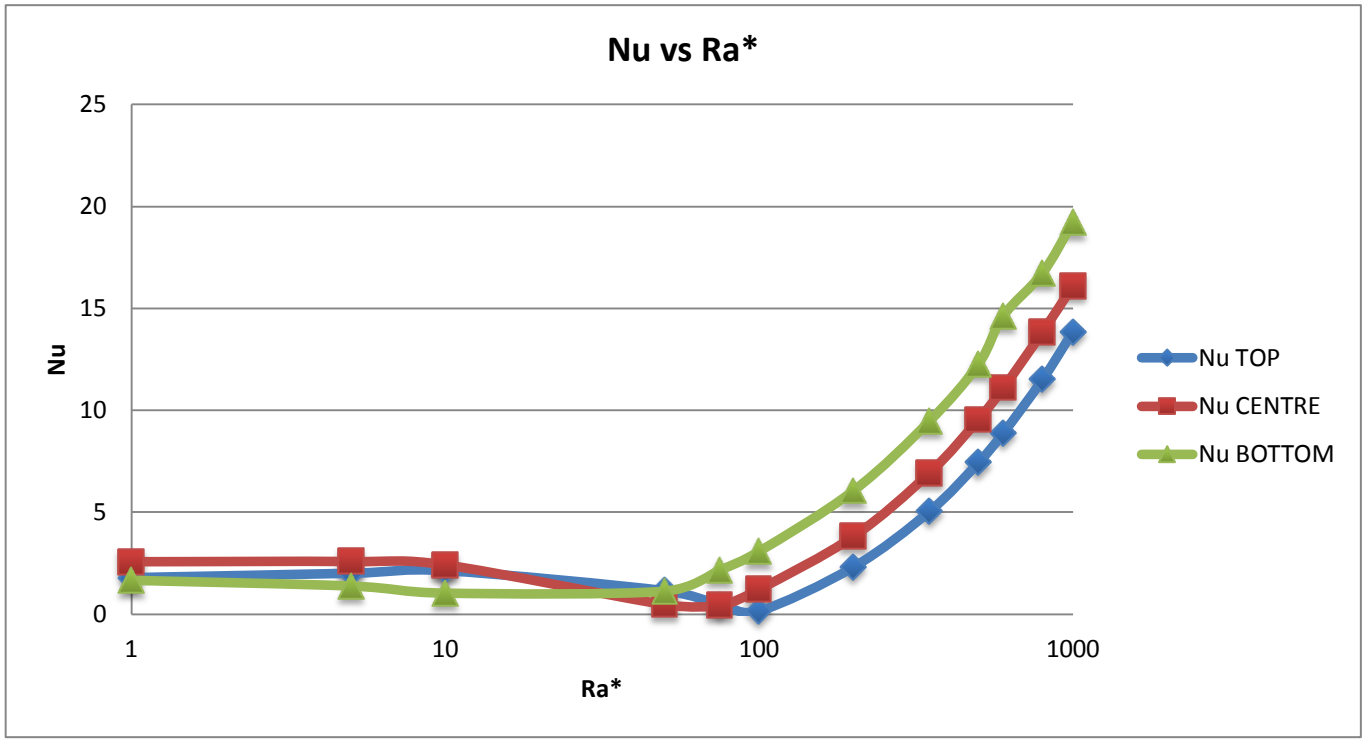

Fig 4a. Nusselt number vs Rayleigh-Darcy number for Non-dimensional heat generation of 0.1(AR=1, Radr=1) buoyancy ratio=0.

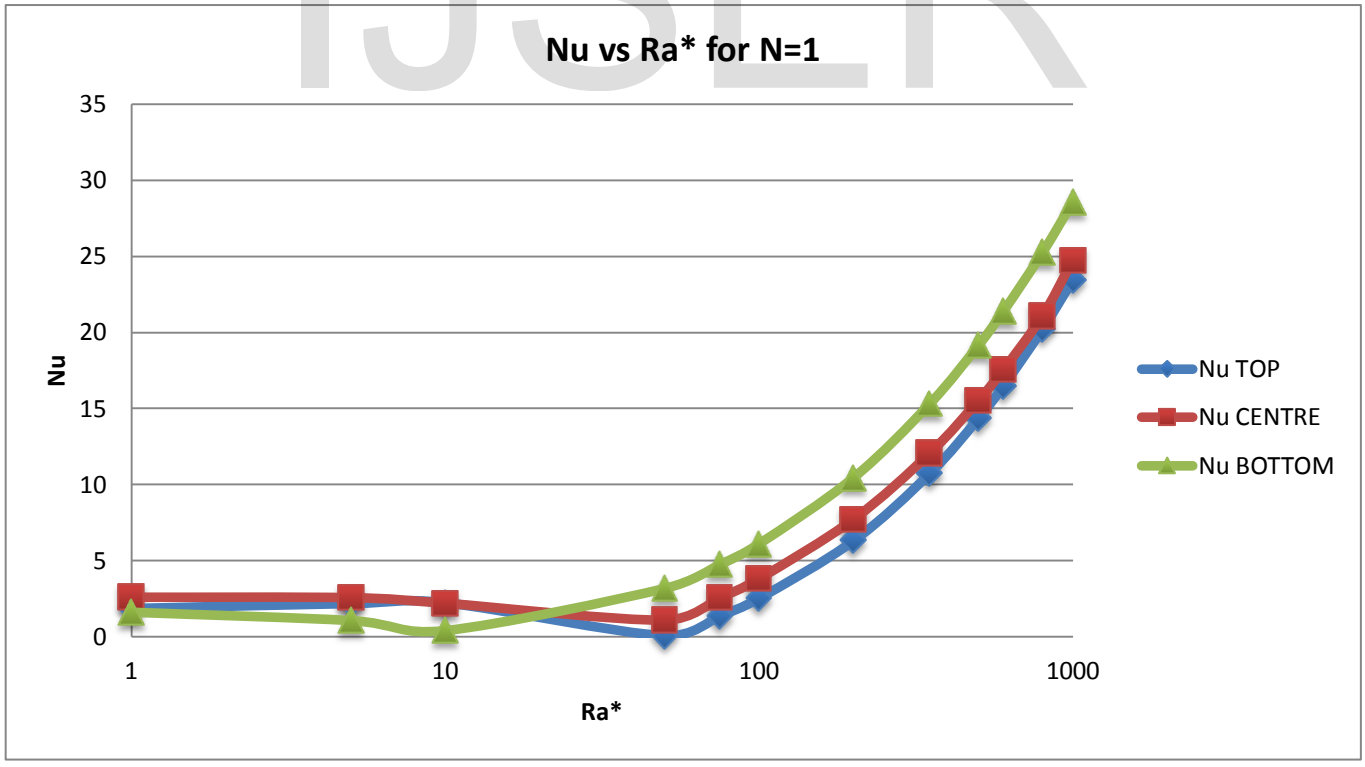

Fig 4b. Nusselt number vs Rayleigh-Darcy number for Non-dimensional heat generation of 0.1(AR=1, Radr=1) buoyancy ratio=1.

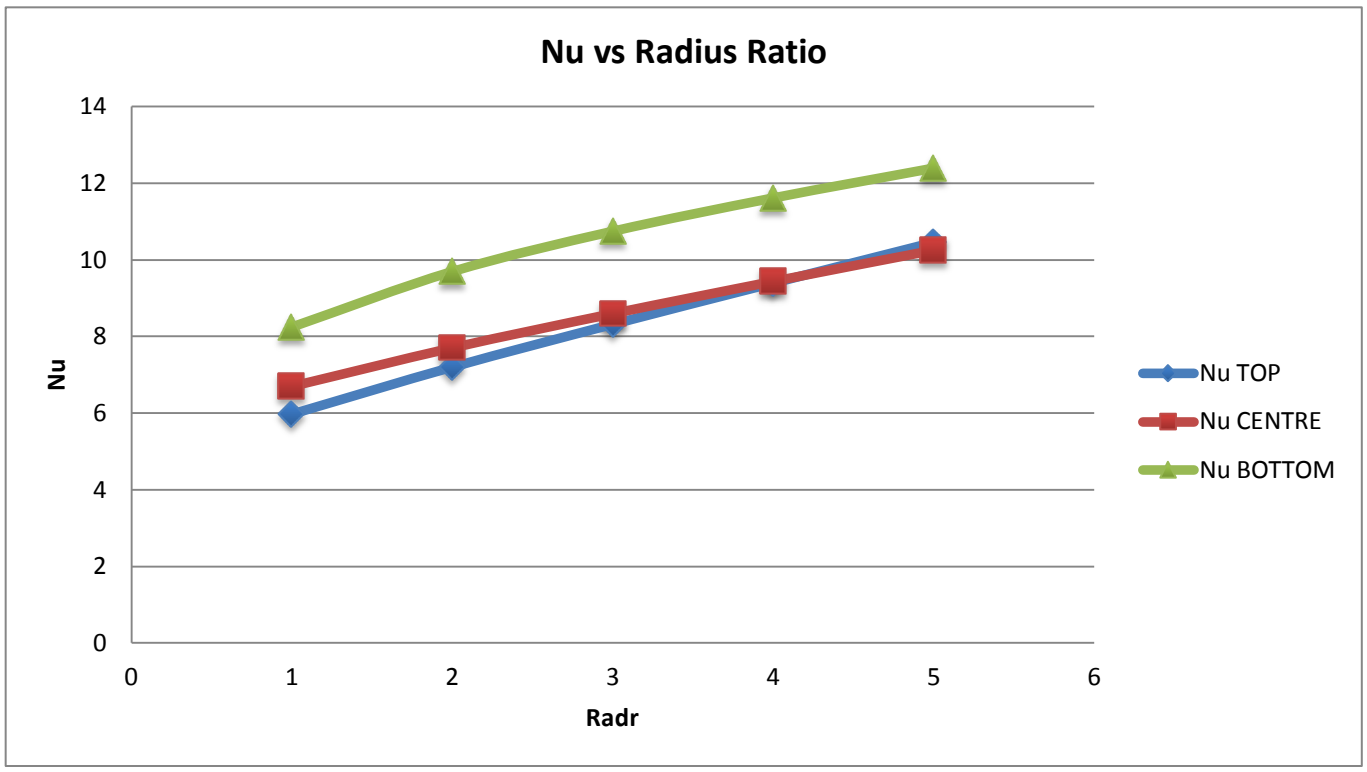

Fig 5. Nusselt number vs Radius ratio for GG=0.1(Ra*=600, AR=5)

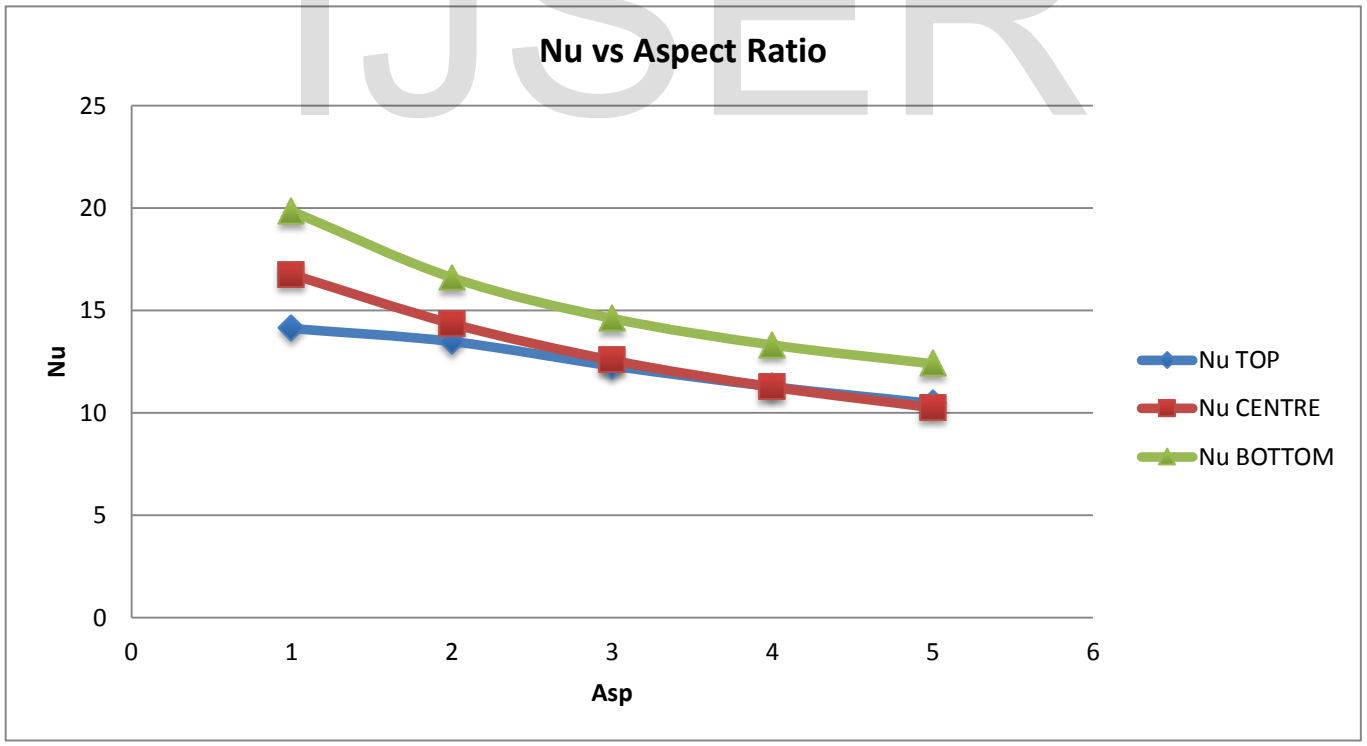

Fig 6. Nusselt number vs Aspect ratio for GG=0.1(Ra*=600, Radr=5)

Fig. 7 shows the streamline plots for various Ra* values considering heat generation on the top, the centre and the bottom. In each of the three cases, for a low Rayleigh-Darcy number, the centre of fluid circulation was found to be close to the middle of the cavity. Fluid in contact with hot wall becomes less dense and moves up. It is replaced by cooler fluid and the cycle continues. As Rayleigh- Darcy number was increased, buoyancy induced flow became dominant and convection was found to increase leading to the flow penetrating deeper into the matrix. Higher Rayleigh-Darcy numbers imply a higher permeability of the solid-porous matrix, providing reduced resistance induced by boundary friction associated with the matrix, thereby allowing the fluid to penetrate deeper into the matrix. The position of the eye of the vortex and the nature of the circulation trend were found to be directly dependent on the position of the heat source, as can be seen in the figure.

Fig. 8a shows the Sherwood number variation with respect to the Rayleigh-Darcy number for a value of Non-dimensional heat generation =0.1 in each of the three cases (Aspect Ratio=1, Radius Ratio=1). The Sherwood number variation with respect to the Rayleigh-Darcy number was found to remain almost constant up to Ra*=10 (pure diffusion case at low values of Ra*). As the Rayleigh-Darcy was increased beyond a value of 10, the Sherwood number started increasing exponentially. This indicated that better fluid circulation and higher buoyancy effects in the flow improved the mass transfer rate. The mass transfer rate magnitude and trends in each of the three cases were found to be similar (refer Table 4). This can be attributed to the fact that, even though a change in the position of the heat source has a direct impact on the heat transfer rate, it has very little effect on concentration induced flow, as a result of which, the mass transfer rate was found to be unaffected by a change in the position of the heat source. Fig. 8b depicts the Sherwood number variation with Ra*, for heat generation on the top of the porous wall. For a constant value of Ra*, the Sherwood number was found to increase drastically as Lewis number was increased from 1 to 10. Mass transfer rate due to enhanced flow and higher buoyancy effects improves with a decrease in thermal diffusion.

In fig. 9a, for a constant value of non-dimensional heat generation=0.1, a constant value of aspect ratio=5 and a constant Rayleigh-Darcy number of 600, the average Sherwood number was found to increase with an increase in radius ratio. This result follows from the fact that with increasing radius ratio, the annulus width increases, and the fluid volume associated with the concentration gradients near the inner boundary increases. For a constant value of Radius Ratio, the Sherwood number was found to increase drastically as Lewis number was increased from 1 to 10 as shown in fig. 9b. In both 9a and 9b, the Sherwood number was found to be at its highest when the heat generation zone was located at the bottom of the porous wall. In fig. 9a the mass transfer rate for the case of heat generation at the centre of the porous wall was found to be slightly less than that for the case of heat generation at the top of the porous wall up to a radius ratio value of 3, beyond which the mass transfer rate for the case of heat generation at the centre was found to be higher than the same at the top. In fig. 9b, as the porous width was increased, the Sherwood number was eventually found to be at its maximum for the case of heat generation at the bottom and similar in magnitude for the cases of heat generation at top and the at the centre.

In fig. 10a, it is observed, that, for a constant value of radius ratio and Rayleigh-Darcy number, the average Sherwood number was found to decrease with an increase in aspect ratio. As Aspect ratio increases, the concentration boundary layer increases in thickness due to reduced fluid density, thereby causing reduced mass transfer. In fig. 10a the mass transfer rate for the case of heat generation at the centre of the porous wall was found to be slightly less than that for the case of heat generation at the top of the porous wall, up to a radius ratio value of 3, beyond which the mass transfer rate for the case of heat generation at the centre was found to be higher than the same at the top. Mass transfer rate was again found to increase with an increase in Lewis number as can be seen in fig. 10b. This behaviour has been explained in the next paragraph. Like in fig. 9b, the Sherwood number was eventually found to be at its maximum for the case of heat generation at the bottom and similar in magnitude for the cases of heat generation at the top and the at the centre.

Fig. 11a depicts the variation of the Average Sherwood Number with increase in Lewis number, for Non-dimensional heat generation of 0.1; AR=5; Radr=5 and Ra*=500. Sherwood number was found to increase with an increase in Lewis number. The concentration boundary layer becomes thinner as Le increases, which in turn increases the concentration gradient and thus the Sherwood number. A logarithmic plot of this

variation is shown in Fig. 11b. A best-fit line was obtained, and using the power law method, one was able to derive a correlation between the Sherwood number and Lewis number. There was an excellent agreement between the values obtained using our correlation and the values from our program. This can be seen in Table 5.

STREAMLINE PLOTS OBTAINED FOR GG=0.1, Radr=Asp=1 at various Rayleigh-Darcy numbers:

TOP:

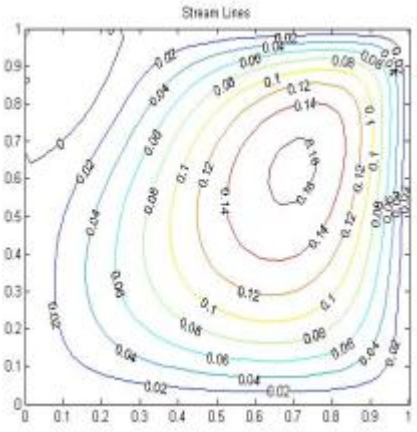

Ra*=1

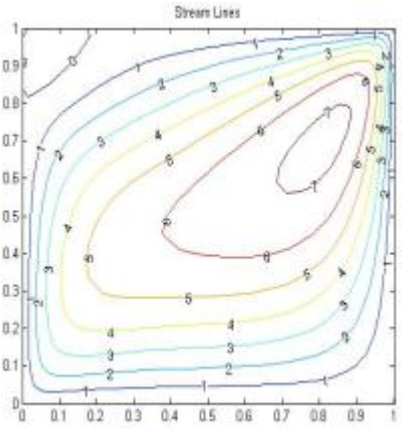

Ra*=100

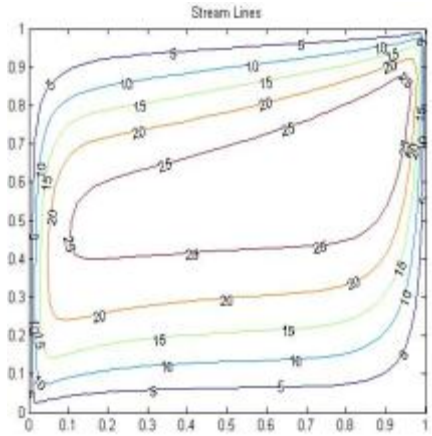

Ra*=1000

CENTRE:

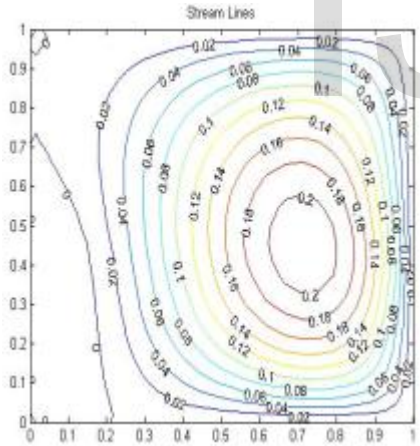

Ra*=1

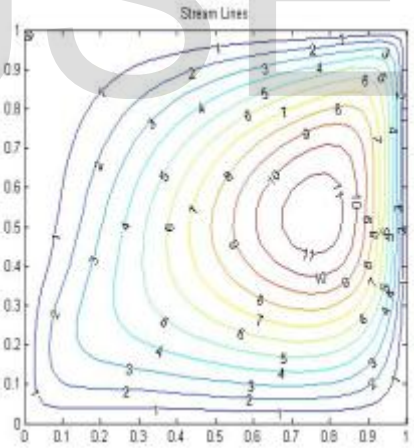

Ra*=100

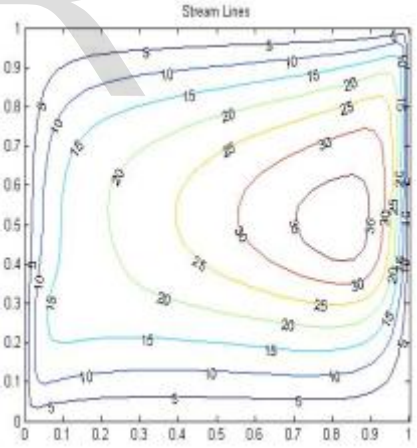

Ra*=1000

BOTTOM:

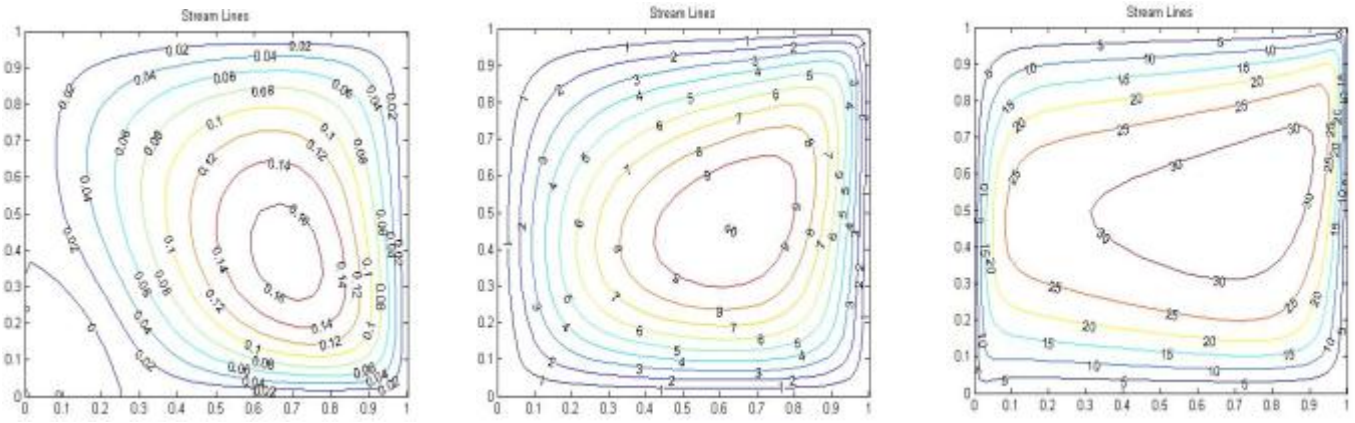

Ra*=1 Ra*=100 Ra*=1000

Fig. 7 Streamline plots obtained for various Ra* values, considering heat generation on the top, the centre and the bottom.

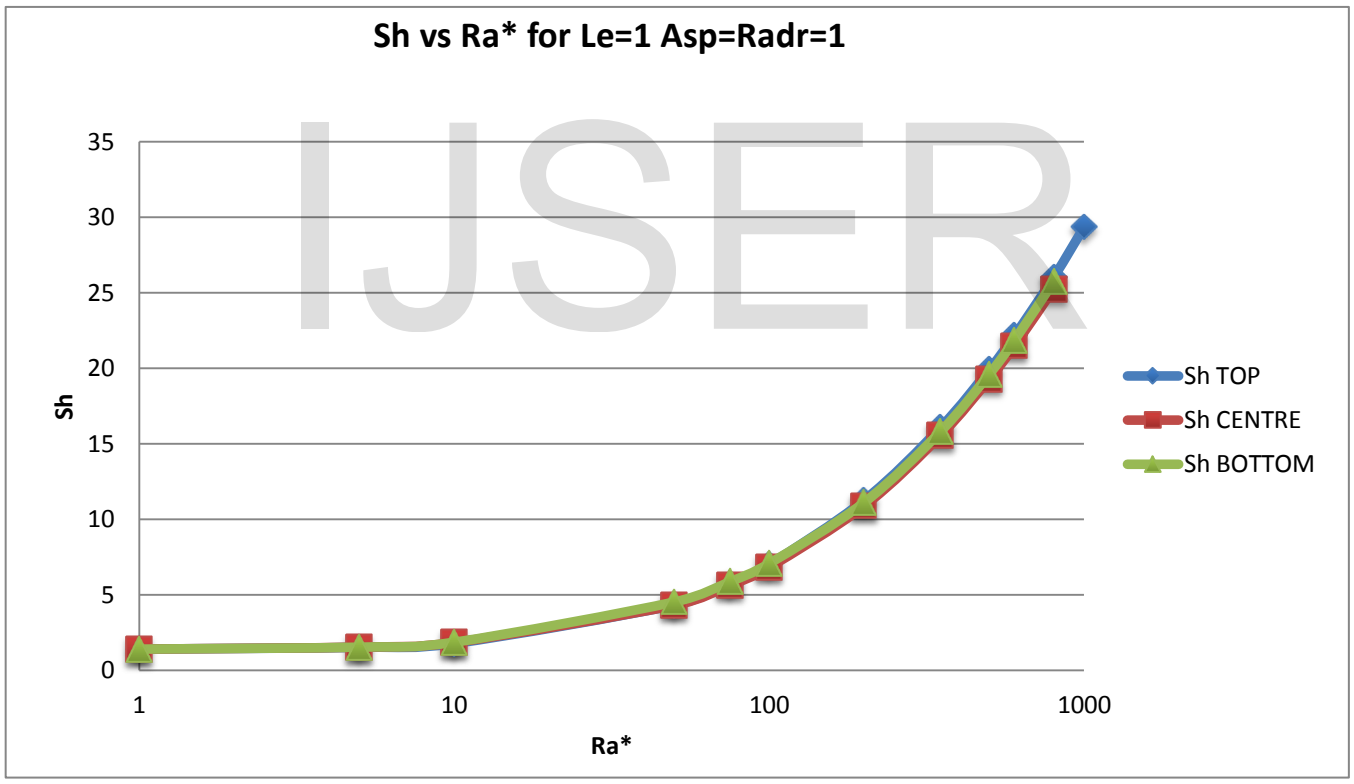

Fig 8a. Sherwood number vs Rayleigh-Darcy number for Non-dimensional heat generation of 0.1(AR=1, Radr=1) in each of the three cases.

Table 2

Ra*	Sh TOP	Sh CENTRE	Sh BOTTOM
1	1.4014	1.4001	1.3992
5	1.5176	1.5352	1.5308
10	1.7772	1.8417	1.859
50	4.315	4.3017	4.5227
75	5.7335	5.6199	5.8664
100	7.0184	6.825	7.0737
200	11.2617	10.8742	11.1092
350	16.0905	15.552	15.8172
500	19.932	19.2971	19.6249
600	22.1501	21.4654	21.8421
800	26.0268	25.2621	25.7439

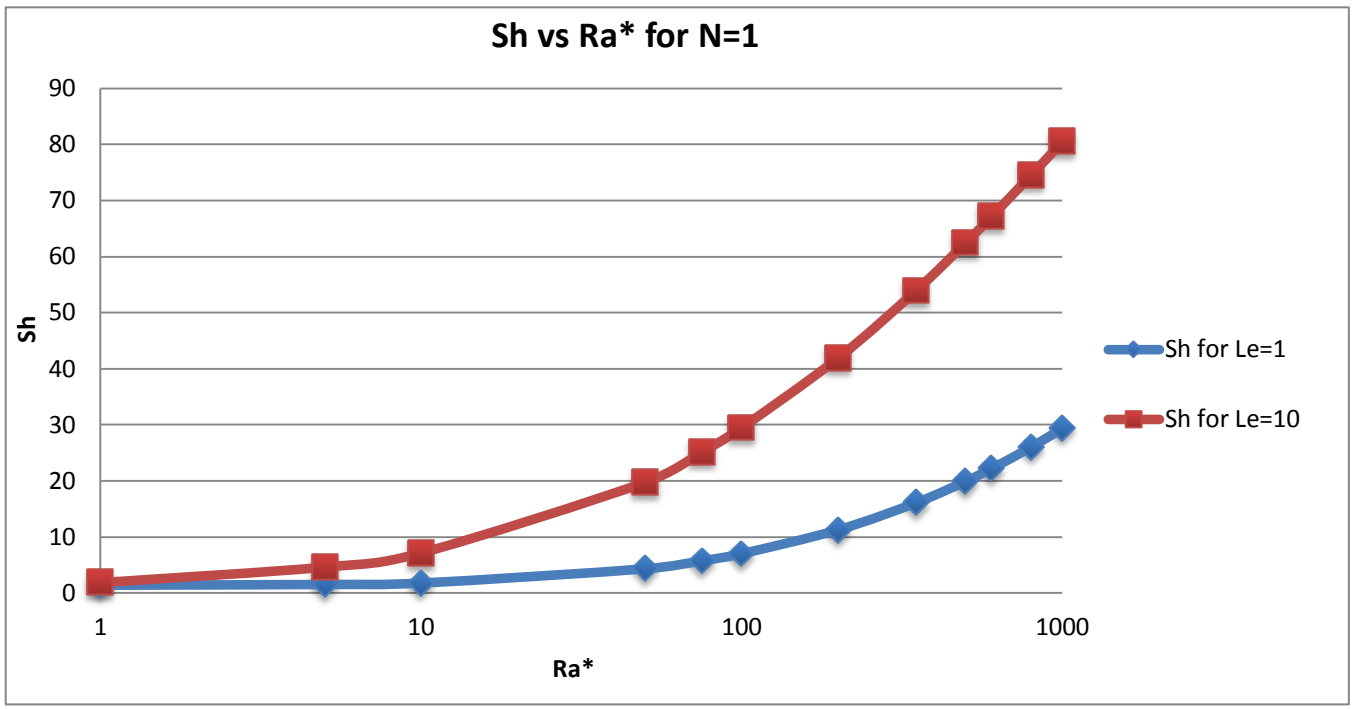

Fig 8b. Sherwood number vs Rayleigh-Darcy number for Non-dimensional heat generation of 0.1 at the top of the porous wall (AR=1, Radr=1) for different values of Lewis number.

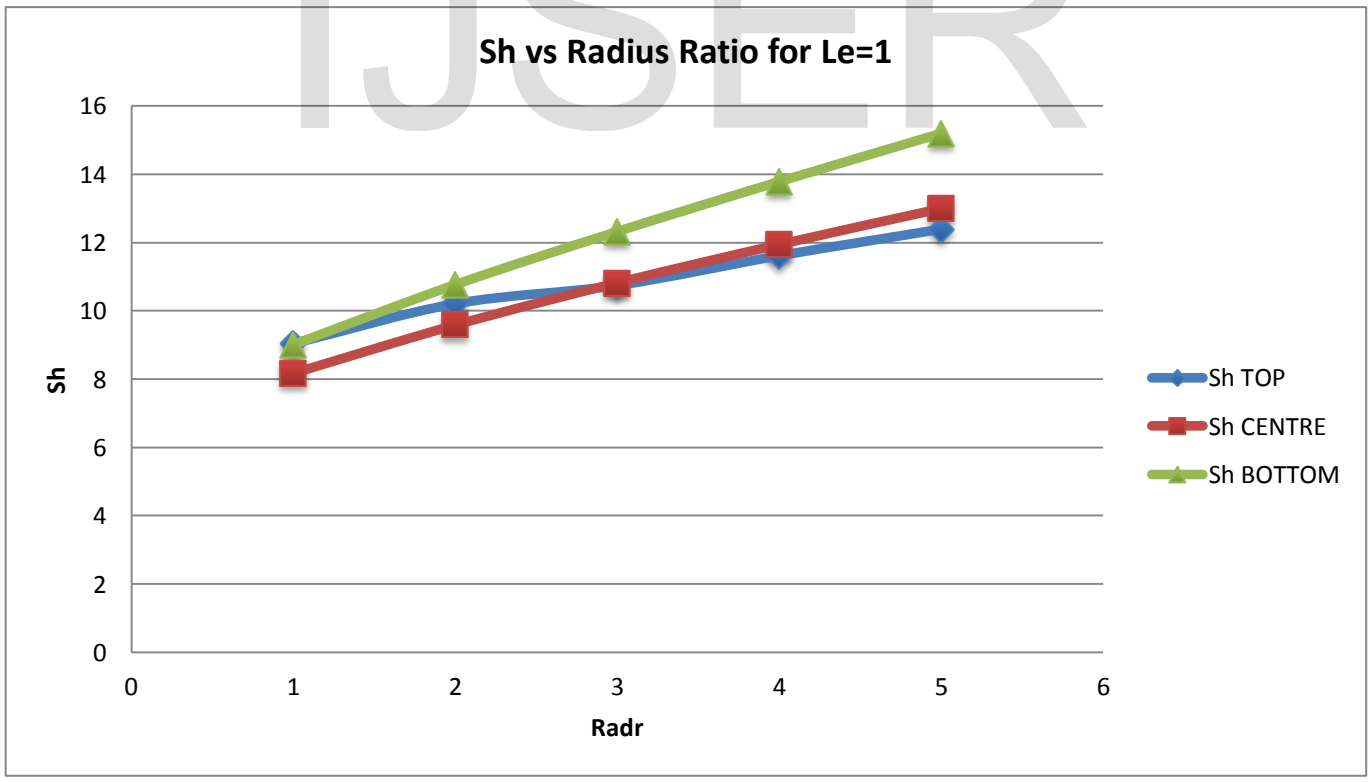

Fig 9a. Sherwood number vs Radius Ratio for Non-dimensional heat generation of 0.1(AR=5, Ra*=600) at Lewis number=1.

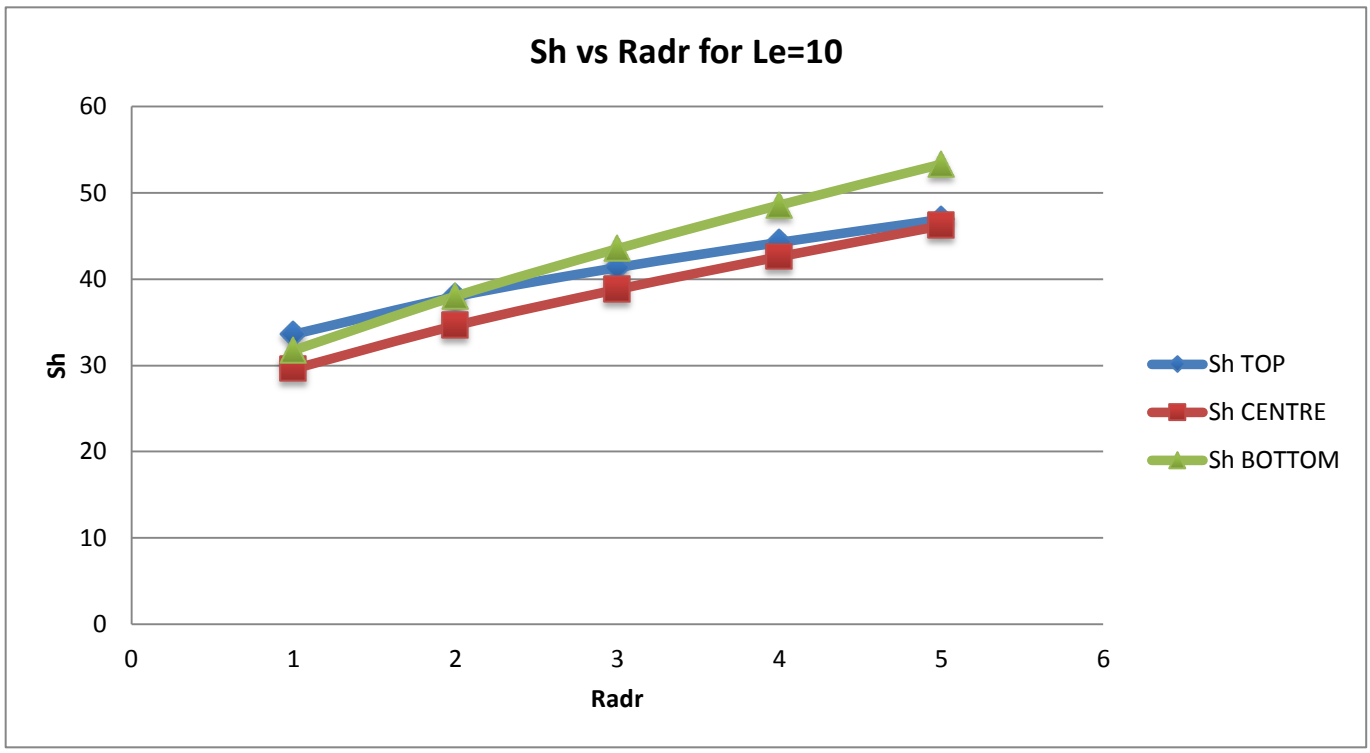

Fig 9b. Sherwood number vs Radius Ratio for Non-dimensional heat generation of 0.1(AR=5, Ra*=600) at Lewis number=10.

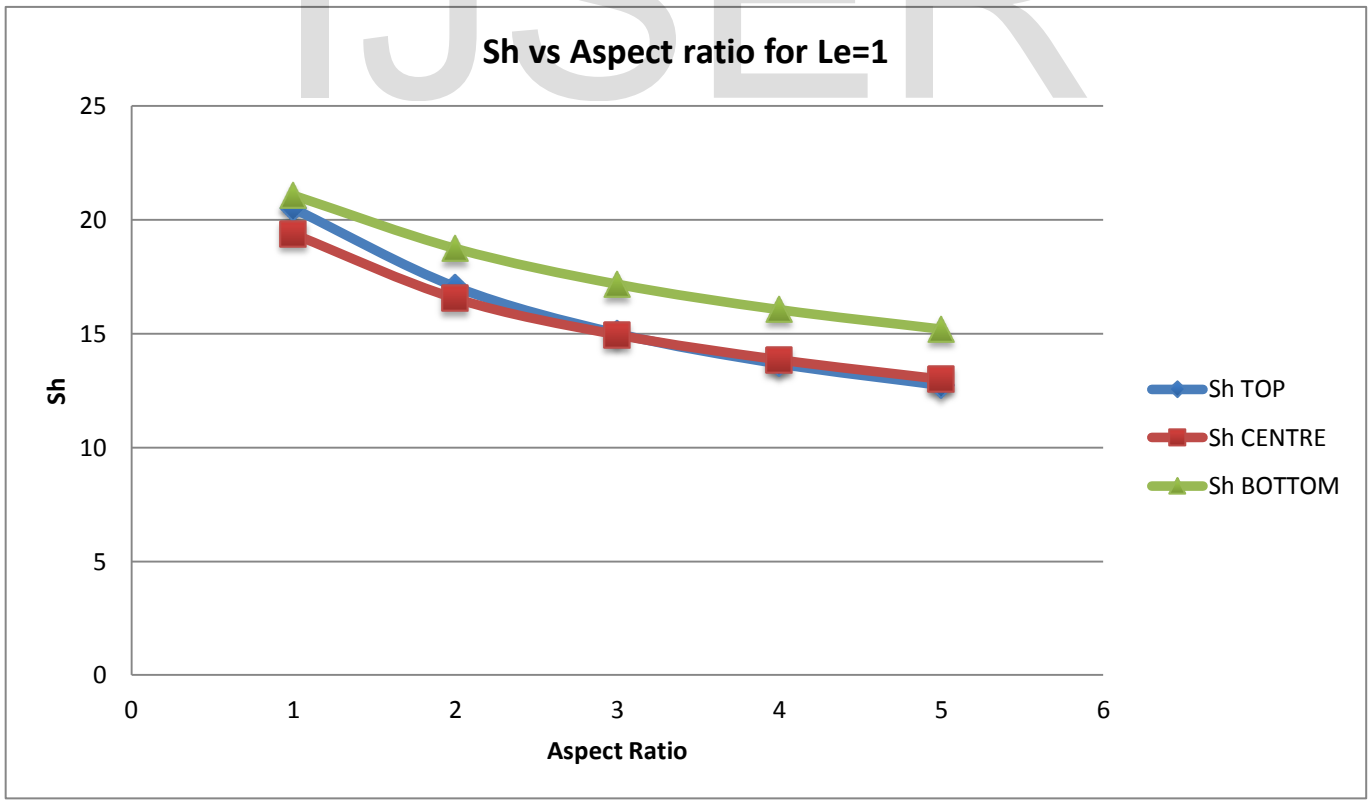

Fig 10a. Sherwood number vs Aspect Ratio for Non-dimensional heat generation of 0.1 (Radr=5, Ra*=600) Lewis number =1.

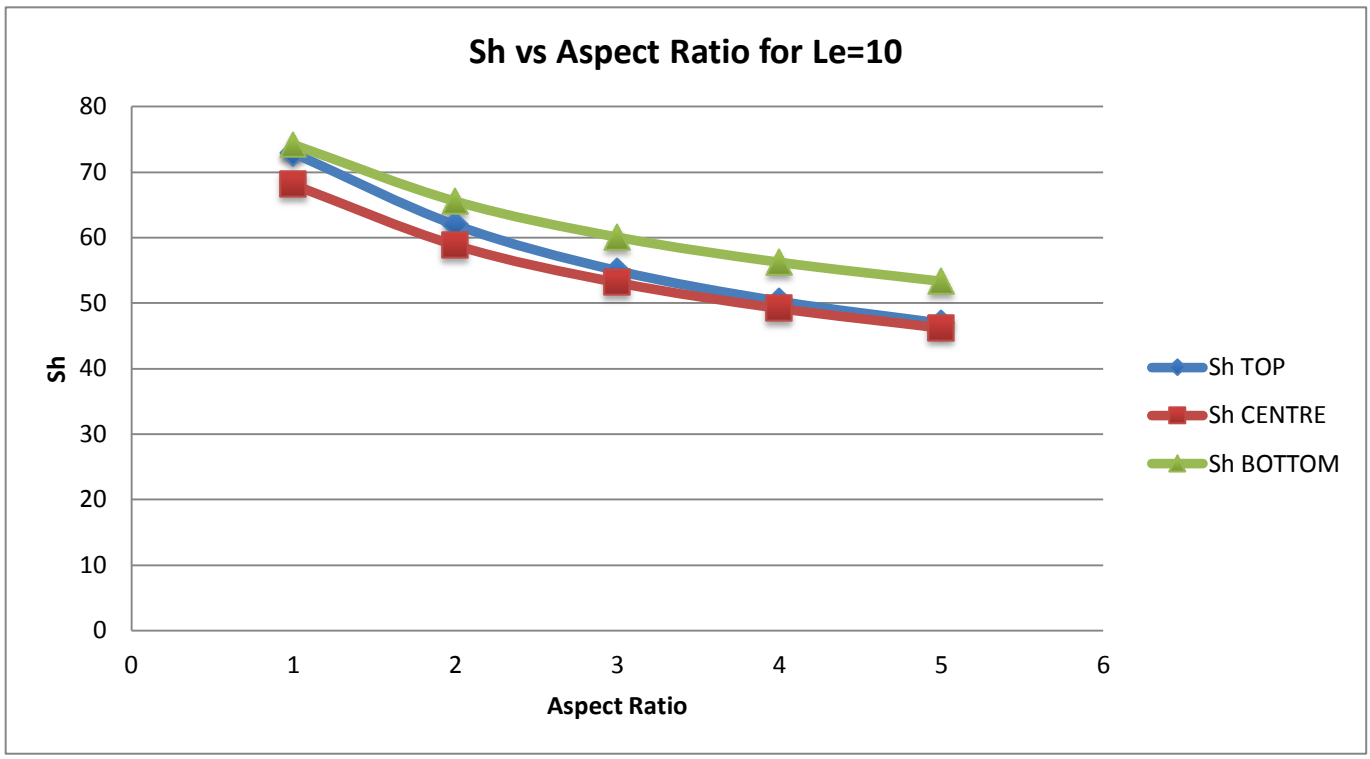

Fig 10b. Sherwood number vs Aspect Ratio for Non-dimensional heat generation of 0.1 (Radr=5, Ra*=600) Lewis number=10.

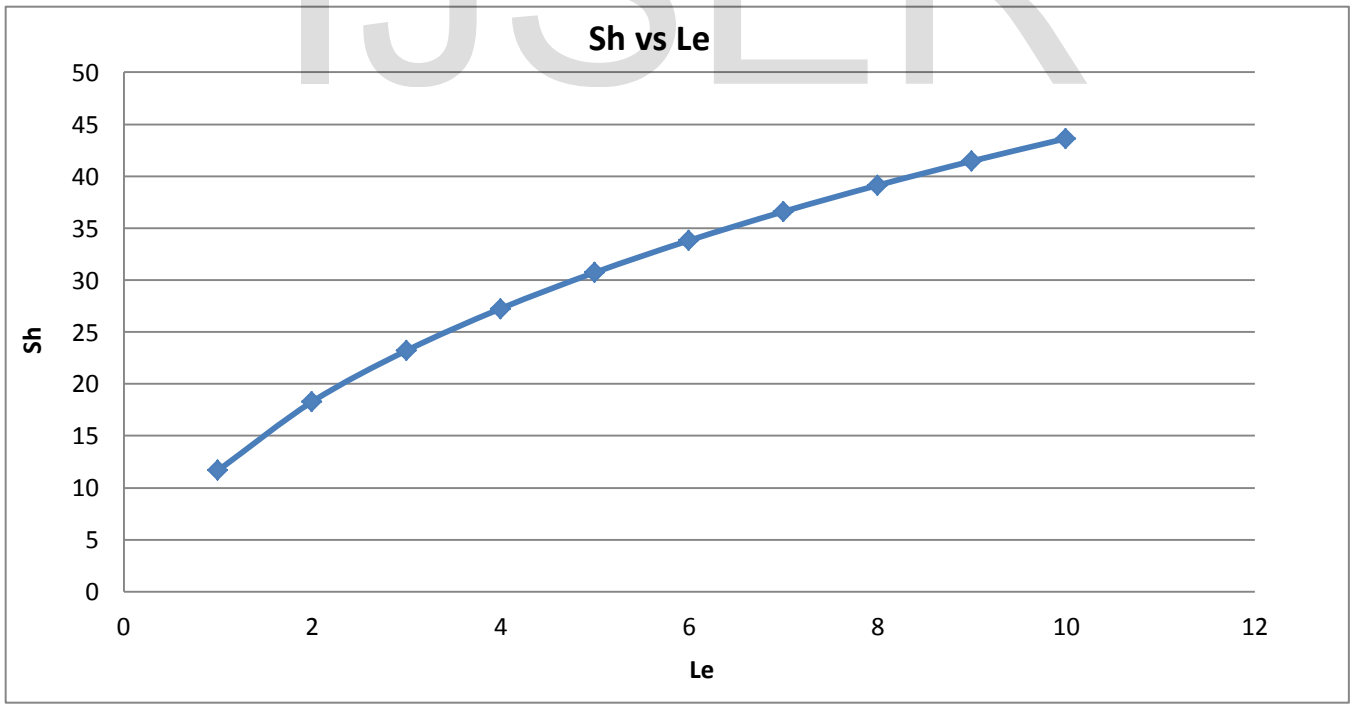

Fig 11a. Sherwood number vs Lewis number for Non-dimensional heat generation of 0.1(AR=5, Radr=5 and Ra*=500).

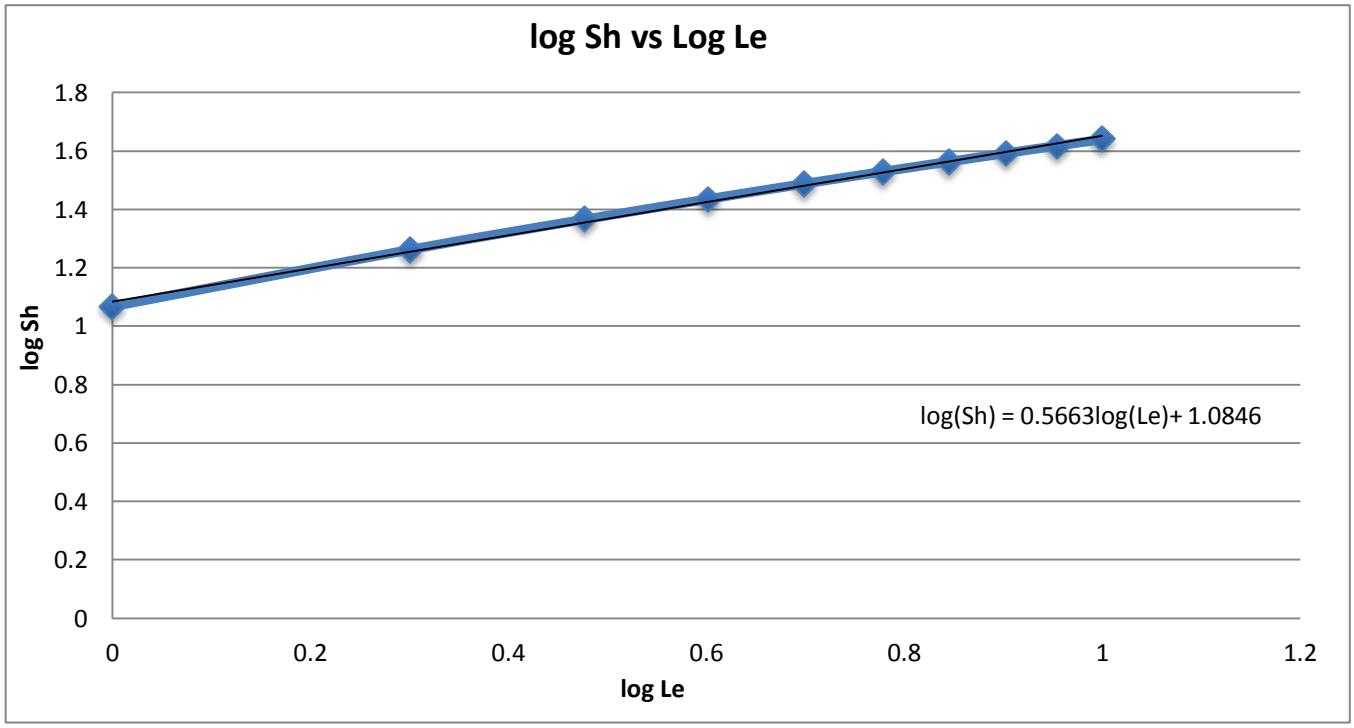

Fig 11b. Logarithmic plot of the Sherwood number vs Lewis number relationship for non-dimensional heat generation of 0.1(AR=5, Radr=5 and Ra*=500).

Table 3

The equation of the best-fit line obtained for the plot shown in fig. 11b. Is:

log(Sh) = 0.5663log(Le)+ 1.0846

Using the Power Law method, one can arrive at a correlation between Sherwood number and Lewis number:

$Sh = 12.1507(Le^{0.5663})$

Le	Sh	Sh correlation
1	11.6804	12.1507
2	18.2988	17.9917
3	23.2172	22.6358
4	27.2567	26.641
5	30.7351	30.2293
6	33.8144	33.5172
7	36.5897	36.5747
8	39.1228	39.4477
9	41.4566	42.1686
10	43.6277	44.7612

Fig. 12 depicts the variation in the iso-concentration lines for various Rayleigh-Darcy numbers for each of the cases studied. One can clearly see how the profile develops from Ra*=10 (pure conduction) to Ra*=1000 (pure convection) -from nearly vertical lines, parallel to the walls to nearly horizontal lines perpendicular to the walls of the cylindrical annulus. The lines were found to accumulate and crowd near the hot wall at higher values of Ra*, indicating the development of a thinner concentration boundary layer and thus, better internal concentration gradients, promoting the mass transfer rate and subsequently improving the value of Sherwood number.

ISOCONCENTRATION PLOTS OBTAINED FOR GG=0.1, Radr=Asp=1 at various Rayleigh-Darcy numbers:

TOP:

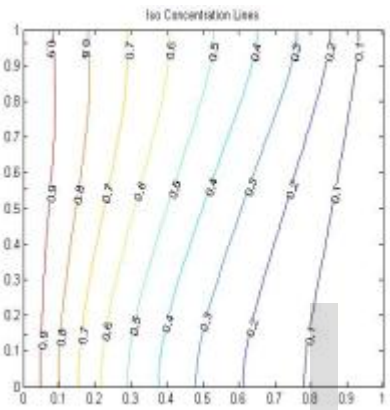

For Ra*=10

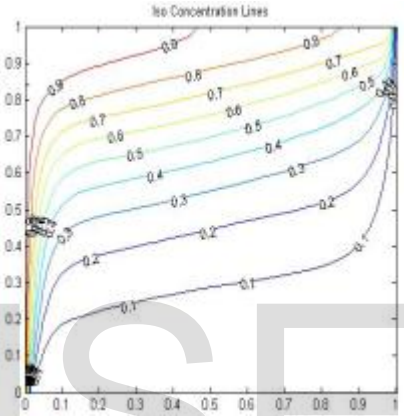

For Ra*=100

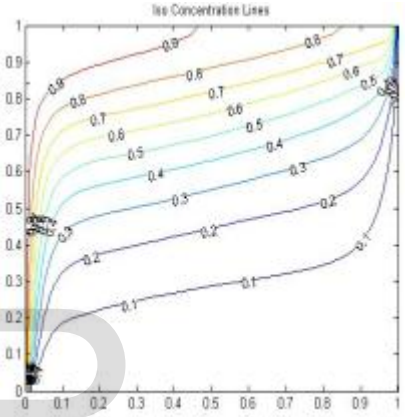

For Ra*=1000

CENTRE:

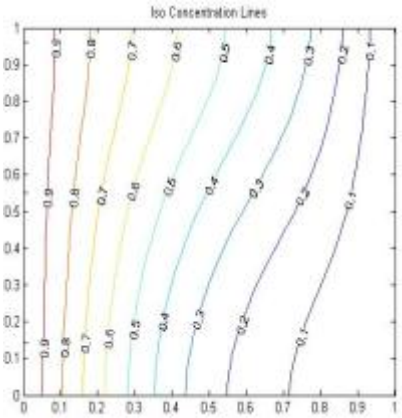

For Ra*=10

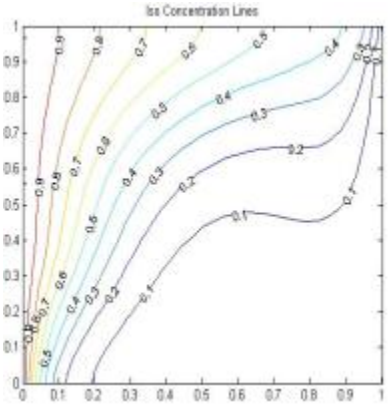

For Ra*=100

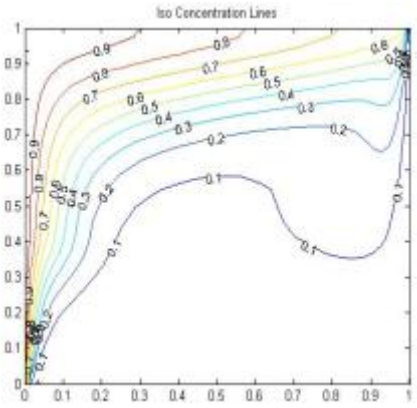

For Ra*=1000

BOTTOM:

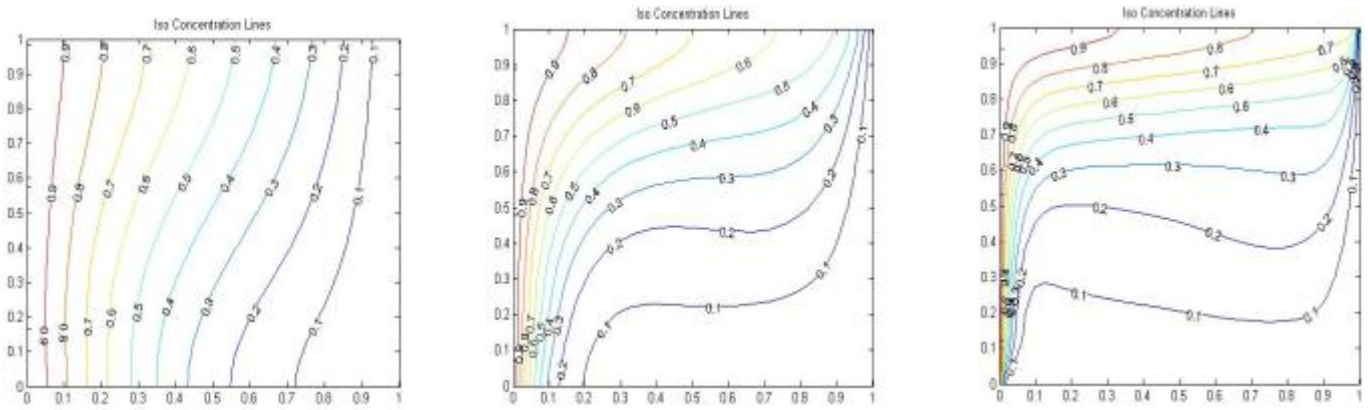

For Ra*=10 For Ra*=100 For Ra*=1000

Fig. 12 Iso-concentration lines for various Ra* values considering heat generation on the top, the centre and the bottom.

5. CONCLUSIONS

Heat and mass transfer in an annular, vertical, porous cylinder was studied considering the thermal equilibrium model for natural convection. Separate heat generation regions were defined: 1.) On the top of the annulus 2.) At the centre of the annulus 3.) At the bottom of the annulus. The Finite Element method was used to obtain the solution for the governing partial differential equations. The following conclusions have been drawn

- Nusselt number was found to increase with an increase in the Rayleigh-Darcy number. This can be attributed to the dominance of the buoyancy effects that arise within the fluid circulation at high Ra* values. Nusselt number was found to be maximum for the case of heat generation at the bottom of the annulus. Nusselt number improved for a positive value of buoyancy ratio.

-Nusselt number was found to increase with an increase in radius ratio due to the development of strong thermal gradients that arise due to an increase in the fluid volume within the annulus. Nusselt number was found to be maximum for the case of heat generation at the bottom of the annulus.

- Nusselt number was found to decrease with an increase in Aspect ratio due to decreased fluid density in higher regions and development of thicker thermal boundary layers leading to smaller thermal gradients. Nusselt number was found to be maximum for the case of heat generation at the bottom of the annulus.

- Sherwood number was found to increase with an increase in the Rayleigh-Darcy number. This can be attributed to the dominance of the buoyancy effects that arise within the fluid circulation at high Ra* values, causing an improvement in the overall mass transfer rate due to better fluid flow within the annulus. The magnitude of the Sherwood number and the corresponding trends in each of the three cases were found to be similar.

-Sherwood number was found to increase with an increase in the radius ratio due to development of strong concentration gradients with an increase in the fluid volume associated with the hot wall. Sherwood number was found to be maximum for the case of heat generation at the bottom of the annulus.

- Sherwood number was found to decrease with an increase in Aspect ratio due to a decrease in the fluid density at the hot wall and therefore thicker concentration boundary layers at the wall causing a drop in the concentration gradients. Sherwood number was found to be maximum for the case of heat generation at the bottom of the annulus.

-Sherwood number was found to increase with increase in Lewis number for a constant Ra* value. As the value of Le increases, thermal diffusion decreases, mass transfer due to enhanced fluid flow becomes dominant, causing a decrease in the concentration boundary layer thickness.

6. REFERENCES

[1] Bejan, A. (1995). Convective Heat Transfer, 2nd edition, New York, John Wiley & Sons,

[2] El Shayeb, M. and Beng, Y. K. (2000). Applications of finite difference and finite element methods for thermal problems, University Malaysia Sabah, Sabah.

[3] Lewis, R.W. Nithiarasu, P. and Seetharamu, K.N. (2004). Fundamentals of the finite element method for heat and fluid flow, John Wiley and sons, Chichester

[4] Nield, D. A. and Bejan, A. (1999). Convection in porous media, 2nd ed, Springer-Verlag..

[5] Segerland, L. J. (1982). Applied finite element analysis. John Wiley and sons, New York.

[6] Vafai K. (2000). Hand book of porous media, Marcel Dekker, New York.

[7] Vafai, K. (2005). Handbook of porous media, second ed, Taylor & Francis Group, Boca Raton.

[8] Clarksean, R. Kwendakwema, N. and Noehm, R. (1988). A study of mixed convection ina porous medium between vertical concentric cylinders, Proceedings of 1988 ASME/AICHe National Heat Transfer Conference. 2: 339-344

[9] Manole, D.M. and Lage, J.L. (1992). Numerical benchmark results for natural convection in a porous medium cavity, in: Heat and Mass Transfer in Porous Media, ASME Conference, HTD 216 55255

[10] Nath, S. K. and Satyamurthy, V. V. (1985). Effect of aspect ratio and radius ratio on free convection heat transfer in a cylindrical annulus filled with porous media, HMT C16-85, Proc. 8th Nat. Heat and Mass Transfer Conf. India, 189-193.

[11] Dr Irfan Anjum Badruddin's Ph.D. thesis "NUMERICAL INVESTIGATION OF HEAT AND MASS TRANSFER IN POROUS MEDIUM FIXED WITH VARIOUS GEOMETRIES".

[12] Badruddin, I., Zainal, Z.A, Narayana, P.A, Seetharamu, K.N, A. Thermal Non Equilibrium modeling of heat transfer through a vertical annulus embedded with porous media. International Journal of Heat and Mass Transfer. 49: (2006) 49552-4965.

[13] B.V.K. Reddy, Arunn Narasimhan. Heat generation effects in natural convection inside a porous annulus. International Communications in Heat and Mass Transfer 37 (2010) 607–610

[14] Abel, S. Prasad, K.V. and Mahaboob, A. (2005).Buoyancy force thermal radiation effects in MHD buodary layer visco-elastic fluid flow over continuously stretching surface. International Journal of Thermal Science. 44: 465-476.

[15] Bahloul, A. (2006). Boundary layer and stability analysis of natural convection in a porous cavity. International Journal of Thermal science. 45:656-663.

[16] Z.G. Du, E. Bilgen, Natural convection in vertical cavities with internal heat generating porous medium, Warme-Stoffubertrag 27 (1992) 149–155.

[17] Havstad, M. A., and Burns, P. J. (1982). Convective Heat Transfer in Vertical Cylindrical Annuli Filled with a Porous Medium, Int. J. Heat Mass Transfer, 25, 1755–1766.

[18] Hickox, C. E., and Gartling, D. K. (1981). A numerical Study ofNatural Convection in a horizontal Porous Layer Subjected to an end-to-end temperature Difference, Int. J. Heat Transfer, 103, 797–802.

[19] C.J. Ho and J.Y. Chang, "A Study of Natural Convection Heat Transfer in a Vertical Rectangular Enclosure with Two-dimensional Heating: Effect of Aspect Ratio", International Journal of Heat and Mass Transfer, 37(6) (1994), pp. 917–925.

[20] Nithiarasu, P., Seetharamu, K.N., Sundararajan, T.: Non-Darcy double-diffusive natural convection in axisymmetric fluid saturated porous cavities. Heat Mass Transf. 32, 427–433 (1997)

[21] N.J. Salman Ahmed, Irfan Anjum Badruddin, Jeevan Kanesan, Z.A. Zainal, K.S. Nazim Ahamed, Study of mixed convection in an annular vertical cylinder filled with saturated porous medium, using thermal non-equilibrium model, International Journal of Heat and Mass Transfer, Volume 54, Issues 17 18, August 2011, Pages 3822-3825